

Nondivergent and negative susceptibilities around critical points of a long-range Hamiltonian system with two order parameters

Yoshiyuki Y. Yamaguchi* and Daiki Sawai

Department of Applied Mathematics and Physics, Graduate School of Informatics, Kyoto University, 606-8501, Kyoto, Japan

The linear response is investigated in a long-range Hamiltonian system from the view point of dynamics, which is described by the Vlasov equation in the limit of large population. Due to existence of the Casimir invariants of the Vlasov dynamics, an external field does not drive the system to the forced thermal equilibrium in general, and the linear response is suppressed. With the aid of a linear response theory based on the Vlasov dynamics, we compute the suppressed linear response in a system having two order parameters, which introduce the conjugate two external fields and the susceptibility matrix of size two accordingly. Moreover, the two order parameters bring three phases and the three types of second-order phase transitions between two of them. For each type of the phase transitions, all the critical exponents for elements of the susceptibility matrix are computed. The critical exponents reveal that some elements of the matrices do not diverge even at critical points, while the mean-field theory predicts divergences. The linear response theory also suggests appearance of negative off-diagonal elements, in other words, an applied external field decreases the value of an order parameter. These theoretical predictions are confirmed by direct numerical simulations of the Vlasov equation.

PACS numbers: 05.20.Dd, 05.70.Jk, 74.25.N-

I. INTRODUCTION

The phase transition is one of the central issues in the field of many-body systems. It is classified into some universality classes, and in particular, the mean-field universality class is easily understood by the Landau's phenomenological theory [1]. Nevertheless, a new aspect of the mean-field universality class is recently revealed by considering dynamics.

Dynamics of the mean-field class, including the systems having long-range interaction [2–4], is described by the VLF's equation, or the collisionless Boltzmann equation, in the limit of large population [5–8]. The Vlasov equation has the infinite number of Casimir invariants, and these invariants may prevent the system from relaxing to thermal equilibrium. Indeed, when the initial state has different values of the Casimir invariants from ones in thermal equilibrium, then the relaxation is impossible. We note that, with finite population, the finite-size fluctuation plays the role of collision and drives the system to thermal equilibrium, while the relaxation time gets longer as the population increases [9–15].

The Casimir invariants hold even when an external field is applied, and the invariants suppress the response [16, 17]. This suppression may induce reduction of the critical exponent for the linear response in the Vlasov dynamics. In a ferromagnetic body, the critical exponents γ_{\pm} of susceptibility χ are defined as $\chi \propto \tau^{-\gamma_{\pm}}$ around the second order phase transition. Here τ is the parameter distance from the critical point like $|T - T_c|$ with temperature T and its critical value T_c , and γ_+ (γ_-) is defined in the paramagnetic (ferromagnetic) phase. The classical values of γ_{\pm} in the mean-field universality class are $\gamma_{\pm} = 1$. However, in

the Vlasov dynamics of the Hamiltonian mean-field (HMF) model [18, 19], which is a paradigmatic toy model of a ferromagnetic body in the mean-field class, the linear response theory gives $\gamma_+ = 1$ [20, 21] but $\gamma_- = 1/4$ [22]. The nonclassical critical exponent is not restricted in the HMF model, and the universality is discussed for spatially periodic one-dimensional systems [23].

In the HMF model, detection of nonclassical critical exponents is extended to the nonlinear response at the critical point [24] and to the correlation length [25], which is generalized to the infinite-range models by introducing the coherent number of particles [26, 27]. Interestingly, the nonclassical critical exponents share some scaling relations with the classical critical exponents.

Another direction of detecting nonclassical critical exponents is to consider the linear response in extended models. In this article, we consider the so-called generalized Hamiltonian mean-field (GHMF) model [28]. In the HMF model, particles are confined on the unit circle, and interaction potential consists of the spatial first Fourier mode only. Introducing the second Fourier mode, the GHMF model acquires the Nematic phase in addition to the paramagnetic (Para) and the ferromagnetic (Ferro) phases. As a result, the GHMF model has the new two phase transitions: the Para-Nematic and the Nematic-Ferro phase transitions. As observed in the HMF model, the critical exponents in the Vlasov dynamics may differ between the two sides of a phase transition, and hence we need to consider six sides for the three phase transitions. Moreover, the susceptibility in one side is described by a 2×2 matrix, since the three phases are characterized by the two order parameters corresponding to the two Fourier modes and each order parameter has the conjugate external field. Consequently, we must consider 6 critical exponent matrices of the size 2×2 and the total number of γ is 24 accordingly.

Appearance of the Nematic phase and the matrix form of the susceptibility give natural questions: Does the appear-

* yyama@amp.i.kyoto-u.ac.jp

ance of the Nematic phase drastically change the critical exponents from the HMF model? Are there any differences in the off-diagonal elements of the critical exponent matrix between the mean-field theory and the Vlasov dynamics? The purpose of this paper is to answer to these questions. We compute the 24 critical exponents theoretically by using a response theory based on the Vlasov dynamics [23], and confirm theoretical predictions by performing direct numerical simulations of the Vlasov dynamics. In the HMF model the reduction of the critical exponent is observed, but we show a stronger result in the GHMF model that some elements of the susceptibility matrices do not diverge at the critical point, even they diverge in the mean-field theory. Further, close to the critical point, we demonstrate that the off-diagonal elements of susceptibility matrix become negative in the Ferro side of the Para-Ferro phase transition.

This article is constructed as follows. The GHMF model and the three phases are introduced in Sec.II with the corresponding Vlasov equation. Responses in statistical mechanics and in the Vlasov dynamics are derived in Secs.III and IV, respectively. Theoretical predictions are examined numerically in Sec.V. The last section VI is devoted to a summary and discussions.

II. GENERALIZED HAMILTONIAN MEAN-FIELD MODEL

A. The model

The GHMF model represents particles confined on the unit circle and is described by the Hamiltonian

$$H_N = \sum_{j=1}^N \frac{p_j^2}{2} + \frac{1}{2N} \sum_{j,k=1}^N \Phi(q_j - q_k) - \sum_{a=1}^2 h_a \sum_{j=1}^N \cos a q_j. \quad (1)$$

The position of j -th particle is $q_j \in (-\pi, \pi]$, and $p_j \in \mathbb{R}$ is the conjugate momentum. h_1 and h_2 represent strength of the external fields. The interaction potential Φ is

$$\Phi(q) = 1 - \Lambda_1 \cos q - \Lambda_2 \cos 2q \quad (2)$$

where Λ_1 and Λ_2 are non-negative constants. Setting $\Lambda_1 = 1$ and $\Lambda_2 = 0$, and restricting $h_2 = 0$, the GHMF model results to the HMF model with the external field h_1 . The coefficients are originally defined as $\Lambda_1 = \Delta$ and $\Lambda_2 = 1 - \Delta$ with $\Delta \in [0, 1]$ to ensure the attractive interaction, but we slightly restrict the parameter interval as $\Lambda_1 \in (0, 1)$ and $\Lambda_2 = 1 - \Lambda_1 \in (0, 1)$ for later convenience. Corresponding to the two Fourier modes in $\Phi(q)$, the two order parameter vectors are defined as

$$\frac{1}{N} \sum_{j=1}^N (\cos q_j, \sin q_j), \quad \frac{1}{N} \sum_{j=1}^N (\cos 2q_j, \sin 2q_j), \quad (3)$$

but we may set the sine parts to be zeros from the rotational symmetry of the system and omit them accordingly. The remaining parts,

$$M_1 = \frac{1}{N} \sum_{j=1}^N \cos q_j, \quad M_2 = \frac{1}{N} \sum_{j=1}^N \cos 2q_j, \quad (4)$$

are conjugate to the external field h_1 and h_2 respectively.

In the limit $N \rightarrow \infty$, dynamics is described by the Vlasov equation

$$\frac{\partial f}{\partial t} + \frac{\partial \mathcal{H}[f]}{\partial p} \frac{\partial f}{\partial q} - \frac{\partial \mathcal{H}[f]}{\partial q} \frac{\partial f}{\partial p} = 0, \quad (5)$$

where the one-particle distribution function $f(q, p, t)$ is defined on the two-dimensional phase space $\mu = (-\pi, \pi) \times \mathbb{R}$. The one-particle Hamiltonian functional $\mathcal{H}[f]$ is defined by

$$\mathcal{H}[f](q, p, t) = \frac{p^2}{2} + \mathcal{V}[f](q, t), \quad (6)$$

where the potential functional is

$$\mathcal{V}[f](q, t) = \int \Phi(q - q') f(q', p', t) dq' dp'. \quad (7)$$

Omitting the sine part in $\mathcal{V}[f]$ again from the rotational symmetry of the system, and introducing the order parameter functionals defined by

$$\mathcal{M}_a[f](t) = \iint_{\mu} \cos a q f(q, p, t) dq dp, \quad (a = 1, 2) \quad (8)$$

the potential functional is rewritten as

$$\mathcal{V}[f](q, t) = 1 - \sum_{a=1}^2 (\Lambda_a \mathcal{M}_a[f](t) + h_a) \cos a q. \quad (9)$$

B. Three phases in unforced equilibrium state

The canonical thermal equilibrium states with zero external fields, $h_1 = h_2 = 0$, are written as

$$f_0(q, p) = \frac{G(H_0, \beta)}{\iint_{\mu} G(H_0, \beta) dq dp}, \quad G(E, \beta) = e^{-\beta E}, \quad (10)$$

where β is the inverse temperature,

$$H_0 = \mathcal{H}[f_0] = \frac{p^2}{2} + V_0(q), \quad (11)$$

and

$$V_0(q) = \mathcal{V}[f_0] = 1 - \Lambda_1 m_{10} \cos q - \Lambda_2 m_{20} \cos 2q. \quad (12)$$

The values of m_{10} and m_{20} are determined by solving the simultaneous self-consistent equations

$$m_{10} = \mathcal{M}_1[f_0], \quad m_{20} = \mathcal{M}_2[f_0]. \quad (13)$$

Note that the right-hand-sides depend on m_{10} and m_{20} through H_0 . We may set m_{10} and m_{20} as non-negative from the rotational symmetry of the system.

The three phases of the GHMF model are characterized as

$$\begin{aligned} \text{Para:} & \quad m_{10} = 0, \quad m_{20} = 0, \\ \text{Nematic:} & \quad m_{10} = 0, \quad m_{20} > 0, \\ \text{Ferro:} & \quad m_{10} > 0, \quad m_{20} > 0. \end{aligned} \quad (14)$$

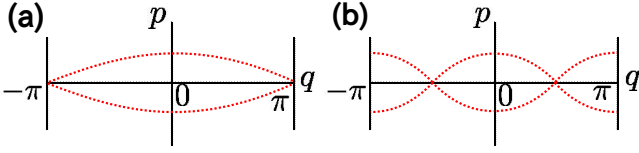


FIG. 1. Schematic pictures of phase space. The red dotted lines represent separatrices. (a) Ferro phase with $m_{10} \gg m_{20}$. (b) Nematic phase.

On the two-dimensional phase space μ , the separatrix is an iso- H_0 contour, and forms the skeleton of the phase space. The Para phase has no separatrix, since the iso- H_0 contours in the Para phase coincide with the iso- p contours. On the other hand, the Ferro and the Nematic phases have separatrices as schematically shown in Fig.1.

III. RESPONSE IN STATISTICAL MECHANICS

Before going to the linear response in the Vlasov dynamics, we revisit the linear response in statistical mechanics for comparison. The Vlasov dynamics corresponds to the microcanonical ensemble, but the microcanonical one gives the equivalent phase diagram with the canonical one except for the parameter region where the first-order phase transition exists [29]. We are interested in the susceptibility around the second-order phase transition, and hence we discuss on the response in the canonical ensemble for simplicity.

The susceptibility is defined in Sec. III A by applying constant external fields, h_1 and h_2 . The critical lines are discussed in Sec. III B based on the divergence of the susceptibility. The critical exponent matrices are obtained in Sec. III C.

A. Susceptibility

Let the system be in the canonical thermal equilibrium state f_0 in the time interval $t < 0$. We apply constant external fields h_1 and h_2 at the time $t = 0$ and wait a long time. Then the system is expected to relax to the forced canonical thermal equilibrium state

$$f^c(q, p) = \frac{G(H^c, \beta)}{\iint_{\mu} G(H^c, \beta) dq dp} \quad (15)$$

with the forced equilibrium Hamiltonian $H^c = \mathcal{H}[f^c]$. The relaxation is not always true in the Vlasov dynamics, but we consider the state $f^c(q, p)$ in this section. The order parameters in f^c are denoted by

$$m_a^c = \mathcal{M}_a[f^c], \quad (a = 1, 2). \quad (16)$$

Expanding the order parameters as

$$m_a^c = m_{a0} + \delta m_a^c, \quad (a = 1, 2), \quad (17)$$

the Hamiltonian H^c is also expanded as

$$H^c = H_0 + \delta V^c \quad (18)$$

with the discrepancy of potential

$$\delta V^c = -(\Lambda_1 \delta m_1^c + h_1) \cos q - (\Lambda_2 \delta m_2^c + h_2) \cos 2q. \quad (19)$$

When the external field $\mathbf{h} = (h_1, h_2)^T$ is small, where the superscript T represents the transposition, the discrepancy δV^c is also small and f^c is expanded as

$$f^c \simeq f_0 - \beta f_0 (\delta V^c - \langle \delta V^c \rangle_0) + O(\|\mathbf{h}\|^2). \quad (20)$$

Here the symbol $\langle X \rangle_0$ represents the average of the observable $X(q, p)$ over f_0 as

$$\langle X \rangle_0 = \iint_{\mu} X(q, p) f_0(q, p) dq dp. \quad (21)$$

Multiplying (20) by $\cos aq$ and integrating over μ , we have the self-consistent equations and their formal solution

$$\delta \mathbf{m}^c = (D^c)^{-1} \beta C^c \mathbf{h}, \quad (22)$$

where the matrix D^c is defined by

$$D^c = \mathbb{1}_2 - \beta C^c \Lambda, \quad (23)$$

the (a, b) -element of the matrix C^c is defined by

$$C_{ab}^c = \langle \cos aq \cos bq \rangle_0 - \langle \cos aq \rangle_0 \langle \cos bq \rangle_0, \quad (24)$$

and

$$\delta \mathbf{m}^c = \begin{pmatrix} \delta m_1^c \\ \delta m_2^c \end{pmatrix}, \quad \mathbb{1}_2 = \begin{pmatrix} 1 & 0 \\ 0 & 1 \end{pmatrix}, \quad \Lambda = \begin{pmatrix} \Lambda_1 & 0 \\ 0 & \Lambda_2 \end{pmatrix}. \quad (25)$$

The susceptibility matrix $\chi^c = (\chi_{ab}^c)$ is defined by

$$\chi_{ab}^c = \lim_{\|\mathbf{h}\| \rightarrow 0} \frac{\partial \delta m_a^c}{\partial h_b}, \quad (26)$$

and the response formula (22) gives

$$\chi^c = (D^c)^{-1} \beta C^c = (D^c)^{-1} (\mathbb{1}_2 - D^c) \Lambda^{-1}. \quad (27)$$

B. Critical lines

Extending the number of order parameters as

$$m_{a0} = \iint_{\mu} \cos aq f_0(q, p) dq dp \quad (a = 3, 4), \quad (28)$$

the matrix C^c is expressed as

$$C^c = \begin{pmatrix} \frac{1 + m_{20}}{2} - m_{10}^2 & \frac{m_{10} + m_{30}}{2} - m_{10} m_{20} \\ \frac{m_{10} + m_{30}}{2} - m_{10} m_{20} & \frac{1 + m_{40}}{2} - m_{20}^2 \end{pmatrix}. \quad (29)$$

	Critical temperature	Critical energy
Para-Ferro	$T = \Lambda_1/2$	$\epsilon_0 = (2 + \Lambda_1)/4$
Para-Nematic	$T = \Lambda_2/2$	$\epsilon_0 = (2 + \Lambda_2)/4$
Nematic-Ferro	$T = \Lambda_1(1 + m_{20})/2$	$\epsilon_0 = \epsilon_{\text{NF}}$

TABLE I. Critical temperature and critical energy of second-order phase transitions. The critical energy of the Nematic-Ferro phase transition is $\epsilon_{\text{NF}} = (2 + \Lambda_1)/4 + m_{20}(\Lambda_1 - 2\Lambda_2 m_{20})/4$.

On the three critical lines, the order parameter m_{10} is always zero, which induces $m_{30} = 0$ by the parity of the mode numbers, and the matrix D^c can be reduced to

$$D^c = \begin{pmatrix} 1 - \beta\Lambda_1 \frac{1 + m_{20}}{2} & 0 \\ 0 & 1 - \beta\Lambda_2 \left(\frac{1 + m_{40}}{2} - m_{20}^2 \right) \end{pmatrix}. \quad (30)$$

The critical point has $\det D^c = 0$, which determines the critical inverse temperature β for fixed Λ_1 and Λ_2 , or the critical parameter Λ_1 (Λ_2) for fixed β and Λ_2 (Λ_1).

The Para-Ferro and the Nematic-Ferro phase transitions are ruled by the order parameter m_{10} , and the Para-Nematic phase transition by m_{20} . Therefore, the critical lines are obtained as

$$\begin{aligned} \text{Para-Ferro: } & 1 - \frac{\beta\Lambda_1}{2} = 0, \\ \text{Nematic-Ferro: } & 1 - \frac{\beta\Lambda_1}{2}(1 + m_{20}) = 0, \\ \text{Para-Nematic: } & 1 - \frac{\beta\Lambda_2}{2} = 0, \end{aligned} \quad (31)$$

where we used the fact that $m_{20} = m_{40} = 0$ on the critical lines of the Para-Ferro and Para-Nematic phase transitions. The value of m_{20} in the Nematic-Ferro phase transition are determined for a given set of β , Λ_1 and Λ_2 by solving the self-consistent equations (13) with $m_{10} = 0$.

Temperature in the canonical ensemble can be transformed to energy in the microcanonical ensemble. The energy functional is defined by

$$\mathcal{E}[f] = \iint_{\mu} \left(\frac{p^2}{2} + \frac{\mathcal{V}[f](q, t)}{2} \right) f(q, p, t) dq dp, \quad (32)$$

where the potential is divided by 2 to avoid the double counting of pair interactions. The value of $\mathcal{E}[f]$ is conserved in the Vlasov dynamics. The unforced equilibrium value of energy $\epsilon_0 = \mathcal{E}[f_0]$ is related to the temperature $T = 1/\beta$ as

$$\epsilon_0 = \frac{T}{2} + \frac{1 - \Lambda_1 m_{10}^2 - \Lambda_2 m_{20}^2}{2}. \quad (33)$$

The critical temperature and the critical energy for a given set of Λ_1 and Λ_2 are arranged in Table I.

C. Critical exponent matrix γ^c

The critical exponent matrix $\gamma^c = (\gamma_{ab}^c)$ is defined by

$$\chi_{ab}^c \propto \tau^{-\gamma_{ab}^c}, \quad (34)$$

	m_{10}	m_{20}	m_{30}	m_{40}
PF	0	0	0	0
FP	$O(\tau^{1/2})$	$O(\tau)$	$O(\tau^{3/2})$	$O(\tau^2)$
PN	0	0	0	0
NP	0	$O(\tau^{1/2})$	0	$O(\tau)$
NF	0	$O(1)$	0	$O(1)$
FN	$O(\tau^{1/2})$	$O(1)$	$O(\tau^{1/2})$	$O(1)$

TABLE II. τ dependence of the spontaneous order parameters m_{10} , m_{20} , m_{30} and m_{40} , where τ is the parameter distance from the critical point. PF and FP represent, for instance, the Para side and the Ferro side of the Para-Ferro phase transition, respectively.

where τ is the parameter distance from the critical point. Looking back (27), we find that the divergences of the susceptibility comes from the inverse matrix $(D^c)^{-1}$, and hence we have to compute τ dependence of the matrix D^c .

For later convenience, we decompose the matrix D^c into the two parts as

$$D^c = A^c + B^c, \quad (35)$$

where

$$A^c = \mathbb{1}_2 - \frac{\beta}{2} \begin{pmatrix} 1 + m_{20} & m_{10} + m_{30} \\ m_{10} + m_{30} & 1 + m_{40} \end{pmatrix} \Lambda \quad (36)$$

and

$$B^c = \beta \begin{pmatrix} m_{10}^2 & m_{10} m_{20} \\ m_{10} m_{20} & m_{20}^2 \end{pmatrix} \Lambda. \quad (37)$$

As shown later, the A part is common to the Vlasov dynamics, but the B part is modified. The estimations of m_{a0} ($a = 1, 2, 3, 4$) are obtained from the self-consistent equations for m_{10} and m_{20} , (13), and from the definitions of m_{30} and m_{40} , (28). The analyses are given in the Appendix A, and the estimated orders are arranged in Table II.

We may assume, around the critical lines, the left-hand-sides of (31) are of $O(\tau)$ in general. This assumption and Table II give estimations of the matrices D^c 's as

$$\begin{aligned} D^c(\text{PF}) &= \begin{pmatrix} O(\tau) & 0 \\ 0 & O(1) \end{pmatrix}, & D^c(\text{FP}) &= \begin{pmatrix} O(\tau) & O(\tau^{1/2}) \\ O(\tau^{1/2}) & O(1) \end{pmatrix}, \\ D^c(\text{PN}) &= \begin{pmatrix} O(1) & 0 \\ 0 & O(\tau) \end{pmatrix}, & D^c(\text{NP}) &= \begin{pmatrix} O(1) & 0 \\ 0 & O(\tau) \end{pmatrix}, \\ D^c(\text{NF}) &= \begin{pmatrix} O(\tau) & 0 \\ 0 & O(1) \end{pmatrix}, & D^c(\text{FN}) &= \begin{pmatrix} O(\tau) & O(\tau^{1/2}) \\ O(\tau^{1/2}) & O(1) \end{pmatrix}, \end{aligned} \quad (38)$$

where NF and FN represent, for instance, the Nematic side and the Ferro side of the Nematic-Ferro phase transition, respectively. We remark that the orders of elements of the matrix B^c are equal to or higher than the matrix A^c , and the matrix B^c is negligible for computing the critical exponent matrices in thermal equilibrium.

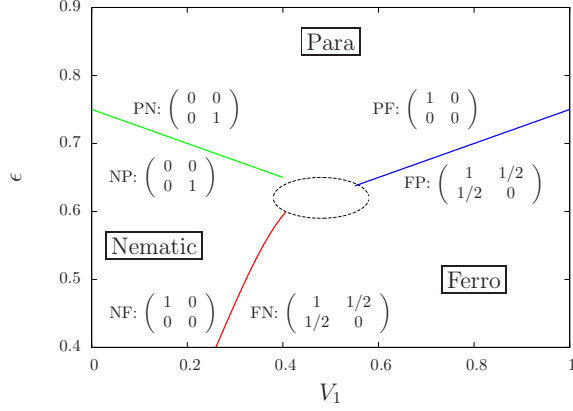


FIG. 2. Phase diagram on (Λ_1, ϵ) plane. $\Lambda_2 = 1 - \Lambda_1$. The region around the black dashed circle includes the first-order phase transition [28, 29], and is out-of-range of the present investigation. The blue right, the green left, and red lower lines are the critical lines of the Para-Ferro, the Para-Nematic and the Nematic-Ferro phase transitions, respectively. In each side of the three phase transitions, the critical exponent matrix γ^c is reported.

Coming back to the formula (27), we have the critical exponent matrices as

$$\begin{aligned} \gamma^c(\text{PF}) &= \begin{pmatrix} 1 & 0 \\ 0 & 0 \end{pmatrix}, & \gamma^c(\text{FP}) &= \begin{pmatrix} 1 & 1/2 \\ 1/2 & 0 \end{pmatrix}, \\ \gamma^c(\text{PN}) &= \begin{pmatrix} 0 & 0 \\ 0 & 1 \end{pmatrix}, & \gamma^c(\text{NP}) &= \begin{pmatrix} 0 & 0 \\ 0 & 1 \end{pmatrix}, \\ \gamma^c(\text{NF}) &= \begin{pmatrix} 1 & 0 \\ 0 & 0 \end{pmatrix}, & \gamma^c(\text{FN}) &= \begin{pmatrix} 1 & 1/2 \\ 1/2 & 0 \end{pmatrix}. \end{aligned} \quad (39)$$

Here we assigned the critical exponent 0 if no divergence appears. These critical exponent matrices are reported in Fig.2 with the critical lines obtained in Sec.III B.

The microcanonical susceptibility does not exceed the canonical susceptibility due to existence of energy conservation [16, 17], but the two types of susceptibility share the critical exponents as shown in the HMF model [22]. See Appendix B for the critical exponents in the microcanonical ensemble.

IV. RESPONSE IN VLASOV DYNAMICS

A nonlinear response theory is recently proposed for the Vlasov systems [24]. Based on it, a simple response formula has been provided [23], which unifies the nonlinear response theory with the linear response theory [20, 21]. The formula is valid under some conditions, but they are satisfied for computing the critical exponents [30]. We first review the formula in Sec.IV A, and the critical exponent matrices are obtained in Sec.IV B. We further discuss on negative elements of a susceptibility matrix in Sec.IV C.

A. Response formula

The setting is the same with the case of thermal equilibrium discussed in Sec.III. The initial state is the unforced thermal equilibrium state f_0 (10) and then a small external field \mathbf{h} is applied at the time $t = 0$. Under the Vlasov dynamics, the state, however, does not go to the forced thermal equilibrium state f^c : it is trapped at a nonequilibrium state denoted by f^V due to the Casimir invariants of the form $\iint_{\mu} s(f) dq dp$, where s is an arbitrary differentiable function. The response formula predicts f^V from f_0 .

The associated one-particle Hamiltonian $H^V = \mathcal{H}[f^V]$ is integrable since f^V is stationary and H^V has one degree of freedom accordingly. The integrability introduces the angle-action variables (θ, J) associated with H^V , and H^V can be written as a function of J only.

Roughly speaking, the response formula is expressed as [23, 24]

$$f^V = \langle f_0 \rangle_{H^V}, \quad (40)$$

where the bracket means the average over the angle variable as

$$\langle X \rangle_{H^V} = \frac{1}{2\pi} \int_0^{2\pi} X(q(\theta, J), p(\theta, J)) d\theta. \quad (41)$$

In other words, f^V is obtained by taking time average of the initial state f_0 under the Hamiltonian flow associated with H^V .

For obtaining the response, as done in Sec.III A, we expand the right-hand-side of (40) with the expansion

$$H^V = H_0 + \delta V^V \quad (42)$$

where

$$\delta V^V = -(\Lambda_1 \delta m_1^V + h_1) \cos q - (\Lambda_2 \delta m_2^V + h_2) \cos 2q. \quad (43)$$

The key idea for expanding the right-hand-side of the formula (40) is to use the equality

$$\langle \varphi(H^V) \rangle_{H^V} = \varphi(H^V) \quad \text{for any } \varphi \quad (44)$$

which holds from the definition of the partial average $\langle \cdot \rangle_{H^V}$. Substituting $H_0 = H^V - \delta V^V$ into the explicit expression

$$\langle f_0 \rangle_{H^V} = \frac{\langle G(H_0, \beta) \rangle_{H^V}}{\iint_{\mu} G(H_0, \beta) dq dp} \quad (45)$$

and expanding the right-hand-side with respect to the small δV^V , we have

$$f^V \simeq f_0 - \beta f_0 \left(\delta V^V - \langle \delta V^V \rangle_{H_0} \right). \quad (46)$$

In the way we performed the expansion again by using $H^V = H_0 + \delta V^V$. The bracket $\langle \cdot \rangle_{H_0}$ is the average over the angle variable associated with H_0 . We omitted a higher order contribution coming from the replacement of $\langle \cdot \rangle_{H^V}$ with $\langle \cdot \rangle_{H_0}$.

Multiplying (46) by $\cos aq$ and integrating over μ , we have a similar formula for susceptibility with thermal equilibrium (27) as

$$\chi^V = (D^V)^{-1} \beta C^V = (D^V)^{-1} (\mathbb{1}_2 - D^V) \Lambda^{-1} \quad (47)$$

but with the different matrix D^V

$$D^V = \mathbb{1}_2 - \beta C^V \Lambda \quad (48)$$

where the (a, b) -element of the matrix C^V is

$$C_{ab}^V = \langle \cos aq \cos bq \rangle_0 - \langle \langle \cos aq \rangle_{H_0} \langle \cos bq \rangle_{H_0} \rangle_0. \quad (49)$$

Here we used the equality

$$\langle \psi_1 \langle \psi_2 \rangle_{H_0} \rangle_0 = \langle \langle \psi_1 \rangle_{H_0} \langle \psi_2 \rangle_{H_0} \rangle_0. \quad (50)$$

The matrix D^V is decomposed into the two parts as

$$D^V = A^c + B^V \quad (51)$$

where the (a, b) -element of the matrix B^V is

$$B_{ab}^V = \beta \langle \langle \cos aq \rangle_{H_0} \langle \cos bq \rangle_{H_0} \rangle_0 \Lambda_b. \quad (52)$$

See the Appendix C for a definite integral formula of each element in a reduced case. The matrix B^V results to the matrix B^c if we replace the partial average over the angle variable, $\langle \cos bq \rangle_{H_0}$, with the average over f_0 , $\langle \cos bq \rangle_0$. However, existence of the partial average modifies the critical exponents.

B. Critical exponent matrix γ^V

According to the Appendix D, the matrices B^V 's are estimated as

$$\begin{aligned} B^V(\text{PF}) &= \begin{pmatrix} 0 & 0 \\ 0 & 0 \end{pmatrix}, & B^V(\text{FP}) &= \begin{pmatrix} O(\tau^{1/4}) & O(\tau^{1/4}) \\ O(\tau^{1/4}) & O(\tau^{1/4}) \end{pmatrix}, \\ B^V(\text{PN}) &= \begin{pmatrix} 0 & 0 \\ 0 & 0 \end{pmatrix}, & B^V(\text{NP}) &= \begin{pmatrix} O(\tau^{1/4}) & 0 \\ 0 & O(\tau^{1/4}) \end{pmatrix}, \\ B^V(\text{NF}) &= \begin{pmatrix} O(1) & 0 \\ 0 & O(1) \end{pmatrix}, & B^V(\text{FN}) &= \begin{pmatrix} O(1) & O(\tau^{c_1}) \\ O(\tau^{c_2}) & O(1) \end{pmatrix}. \end{aligned} \quad (53)$$

The constants c_1 and c_2 in $B^V(\text{FN})$ are positive and we skip to compute their precise values since they do not contribute to the critical exponents as shown later.

As contrasted with thermal equilibrium case, the matrix B^V can partially dominate the matrix D^V . This domination modifies the estimations of D^V 's from D^c 's as

$$\begin{aligned} D^V(\text{PF}) &= \begin{pmatrix} O(\tau) & 0 \\ 0 & O(1) \end{pmatrix}, & D^V(\text{FP}) &= \begin{pmatrix} O(\tau^{1/4}) & O(\tau^{1/4}) \\ O(\tau^{1/4}) & O(1) \end{pmatrix}, \\ D^V(\text{PN}) &= \begin{pmatrix} O(1) & 0 \\ 0 & O(\tau) \end{pmatrix}, & D^V(\text{NP}) &= \begin{pmatrix} O(1) & 0 \\ 0 & O(\tau^{1/4}) \end{pmatrix}, \\ D^V(\text{NF}) &= \begin{pmatrix} O(1) & 0 \\ 0 & O(1) \end{pmatrix}, & D^V(\text{FN}) &= \begin{pmatrix} O(1) & O(\tau^{\tilde{c}_1}) \\ O(\tau^{\tilde{c}_2}) & O(1) \end{pmatrix}, \end{aligned} \quad (54)$$

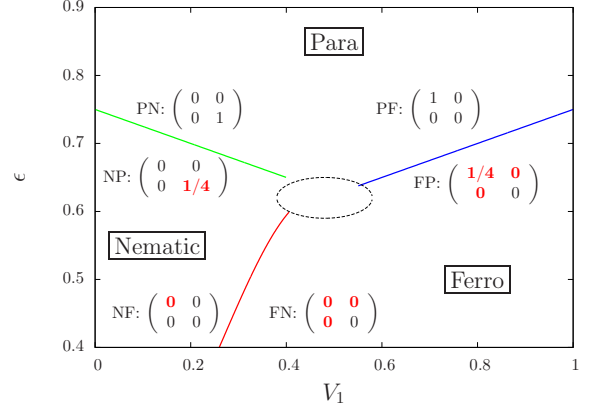


FIG. 3. The same with Fig.2 but the critical exponent matrices are for the Vlasov dynamics, γ^V . The red bold elements are different values from the corresponding equilibrium values.

where $\tilde{c}_j = \min\{1/2, c_j\}$ ($j = 1, 2$). Recalling the susceptibility formula (47), we have the critical exponent matrices γ^V as

$$\begin{aligned} \gamma^V(\text{PF}) &= \begin{pmatrix} 1 & 0 \\ 0 & 0 \end{pmatrix}, & \gamma^V(\text{FP}) &= \begin{pmatrix} 1/4 & 0 \\ 0 & 0 \end{pmatrix}, \\ \gamma^V(\text{PN}) &= \begin{pmatrix} 0 & 0 \\ 0 & 1 \end{pmatrix}, & \gamma^V(\text{NP}) &= \begin{pmatrix} 0 & 0 \\ 0 & 1/4 \end{pmatrix}, \\ \gamma^V(\text{NF}) &= \begin{pmatrix} 0 & 0 \\ 0 & 0 \end{pmatrix}, & \gamma^V(\text{FN}) &= \begin{pmatrix} 0 & 0 \\ 0 & 0 \end{pmatrix}, \end{aligned} \quad (55)$$

where we assigned the critical exponents 0 when no divergences appear even if χ_{ab} 's go to zeros in the limit $\tau \rightarrow 0$. The obtained critical exponent matrices are shown in Fig.3 with stressing the different values from the thermal equilibrium case.

We remark that existence of invariants suppress the response [16, 17], and hence $\chi^V \leq \chi^c$. This fact implies that no critical lines exist on the parameter plane except for the ones obtained in canonical statistical mechanics. Consequently, there are no shifts of the critical lines and the new zero critical exponents correctly capture the dynamical obstacle to divergences of susceptibility at the critical point.

C. Negative susceptibility in the Para-Ferro phase transition

We note that the susceptibility matrix χ is proportional to $D^{-1}(\mathbb{1}_2 - D) = D^{-1} - \mathbb{1}_2$, which is written as

$$D^{-1} - \mathbb{1}_2 = \frac{1}{\det D} \begin{pmatrix} D_{22} - \det D & -D_{12} \\ -D_{21} & D_{11} - \det D \end{pmatrix}. \quad (56)$$

We consider if the signs of the off-diagonal elements can change around the critical point. The sign of $\det D$ must be fixed in one side of a phase transition around the critical line, since $\det D = 0$ appears only on the critical lines. Thus,

we concentrate on the off-diagonal elements of the matrix D by focusing on the Ferro side of the Para-Ferro phase transition.

The off-diagonal elements of D^c (FP) are proportional to

$$-\frac{m_{10} + m_{30}}{2} + m_{10}m_{20}, \quad (57)$$

and are dominated by the negative first term. Thus, no change of sign is possible around the critical point in thermal equilibrium. Indeed, χ_{21}^c (FP) $\rightarrow +\infty$ in the limit $\tau \rightarrow 0$ reflecting the positive critical exponent γ_{12}^c (FP) = 1/2.

However, in the Vlasov dynamics, the off-diagonal elements of D^V (FP), which are proportional to

$$-\frac{m_{10} + m_{30}}{2} + \langle \langle \cos q \rangle_{H_0} \langle \cos 2q \rangle_{H_0} \rangle_0, \quad (58)$$

may change the signs around the critical point. The second term is of $O(\tau^{1/4})$ [see B^V (FP) in (53)], and is positive by considering iso- H_0 contour and f_0 , while the first term is negative and is of $O(\tau^{1/2})$. Thus, the second term can dominate close to the critical point and change the signs of susceptibility. We will numerically demonstrate the negative susceptibility, i.e. χ_{21}^V (FP) < 0 , in Sec.VC.

V. NUMERICAL TESTS

The critical exponents 1/4 of γ_{11}^V (FP) and γ_{22}^V (NP) are direct extensions of the HMF model, whose Ferro phase also has the same critical exponent [22]. γ_{12}^V (FN) = γ_{21}^V (FN) = 0 may associate with γ_{11}^V (FN) = 0. Therefore, interesting exponents are γ_{11}^V (NF) = γ_{11}^V (FN) = 0 and γ_{12}^V (FP) = γ_{21}^V (FP) = 0. We confirm γ_{11}^V (NF) = γ_{11}^V (FN) = 0 in Sec.VA and γ_{21}^V (FP) = 0 in Sec.VB by direct numerical simulations of the Vlasov equation (5). The negative susceptibility discussed in Sec.IV C is also examined in Sec.VC.

We perform the semi-Lagrangian simulations [31] with the fixed time step $\Delta t = 0.05$. The phase space μ is truncated into $(-\pi, \pi] \times [-4, 4]$, and is divided into the grid size $G \times G$. The initial state is the unforced thermal equilibrium state $f_0(q, p)$, (10), and a small external field h_1 is applied with keeping $h_2 = 0$. We compute temporal evolution of the order parameter values $m_1 = \mathcal{M}_1[f]$ and $m_2 = \mathcal{M}_2[f]$ both for $h_1 = 0$ and for $h_1 > 0$, which are denoted by $m_a(t, 0)$ and $m_a(t, h_1)$ ($a = 1, 2$) respectively at the time t . Then, we observe the normalized discrepancy between the two to exclude numerical errors for $h_1 = 0$. That is, we observe the quantities

$$\chi_{a1}(t) = \frac{m_a(t, h_1) - m_a(t, 0)}{h_1}, \quad (a = 1, 2). \quad (59)$$

The family of initial states is characterized by the inverse temperature $\beta = 1/T$, but β is just a parameter and is interpreted as energy by the relation (33). All the simulations are performed for the deterministic Vlasov equation (5), and no thermal noise is introduced.

$$\text{A. } \gamma_{11}^V \text{ (NF)} = \gamma_{11}^V \text{ (FN)} = 0$$

Following the previous work [28], we fix energy as $\epsilon = 0.55$ to avoid the first-order phase transition region, and vary Λ_1 . The parameter τ is, therefore, $\tau = |\Lambda_1 - \Lambda_{1c}|$, where the critical value V_{1c} and the value of m_{20} at the critical point are computed as

$$V_{1c} \simeq 0.358989, \quad m_{20} \simeq 0.518977 \quad (60)$$

for $h_1 = h_2 = 0$. We concentrate on the nondivergence of χ_{11} at the critical point of the Nematic-Ferro phase transition, which implies γ_{11}^V (NF) = γ_{11}^V (FN) = 0.

The (1, 1)-element of the matrix B^V (NF) is expressed in the integral form as

$$B_{11}^V \text{ (NF)} = \frac{\sqrt{2\pi\beta\Lambda_2 m_{20}}}{I_0(\beta\Lambda_2 m_{20})} \int_0^1 e^{-\beta\Lambda_2 m_{20}(2k^2-1)} \frac{k}{K(k)} dk \quad (61)$$

where I_0 is the zeroth order modified Bessel function, and $K(k)$ is the complete elliptic integral of the first kind. $k = 0$ and $k = 1$ correspond to the minimum energy and the separatrix energy respectively. We used the fact that $\langle \cos q \rangle_{H_0} = 0$ in the separatrix outside. See the Appendix C 4 for the derivation of (61). Computing the integral numerically, we have the values of D_{11}^V (NF) and χ_{11}^V (NF) as

$$D_{11}^V \text{ (NF)} \simeq 0.936902, \quad \chi_{11}^V \text{ (NF)} = \frac{1 - D_{11}^V}{\Lambda_1 D_{11}^V} \simeq 0.187603 \quad (62)$$

at the critical point.

The grid size dependence of $\chi_{11}(t)$ is reported in Fig.4, and the numerical results approach to the theoretical level as the grid gets finer. We also computed h_1 dependence of $\chi_{11}(t)$ with the grid size $G = 512$, and the three numerical curves for $h_1 = 10^{-4}, 10^{-5}$ and 10^{-6} almost collapse within the symbol size of Fig.4 (not shown). We, therefore, conclude that the nondivergence of susceptibility and the finite theoretical level (62) are successfully confirmed at the critical point.

$$\text{B. } \gamma_{21}^V \text{ (FP)} = 0$$

To avoid the first-order phase transition region again, we set $\Lambda_1 = 0.8$ and $\Lambda_2 = 0.2$, which gives the critical energy $\epsilon_c = 0.7$, and vary ϵ below the critical point ϵ_c . Thus, the parameter τ is $\tau = \epsilon_c - \epsilon$, since we are in the Ferro, low energy phase. We compute the time averages of $\chi_{11}(t)$ and $\chi_{21}(t)$ in the time window $t \in [200, 1000]$. The averaged susceptibilities are reported in Fig.5 as functions of $\epsilon_c - \epsilon$ for the three Grid sizes, $G = 128, 256$ and 512 . The numerical results are in good agreements with an approximate theory, in which m_{a0} ($a = 2, 3, 4$) are neglected (see the Appendix C for the integral form of each element of the matrix B^c (FP) in this approximated case). The critical exponent γ_{11}^V (FP) = 1/4 is successfully reproduced as in the HMF model [22], and no divergence of χ_{21} to $+\infty$ is also confirmed.

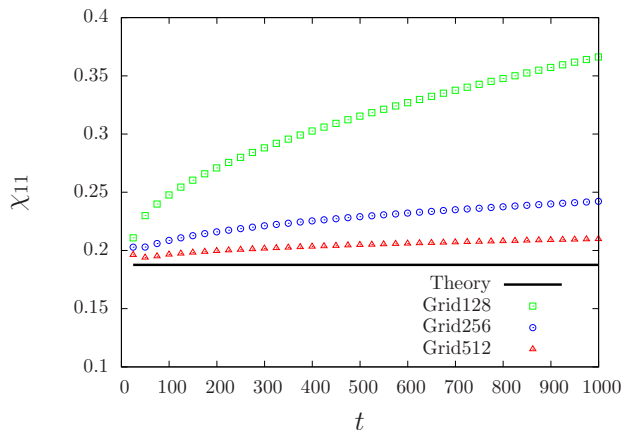


FIG. 4. Temporal evolution of $\chi_{11}(t)$ at the critical point (60) of the Nematic-Ferro phase transition with energy $\epsilon = 0.55$. Initial state is f_0 , [Eq.(10)]. $h_1 = 10^{-4}$ and $h_2 = 0$. The grid sizes are $G = 128$ (green squares), 256 (blue circles) and 512 (red triangles). The black horizontal solid line is the theoretical level of $\chi_{11}^V(\text{NF})$, (62).

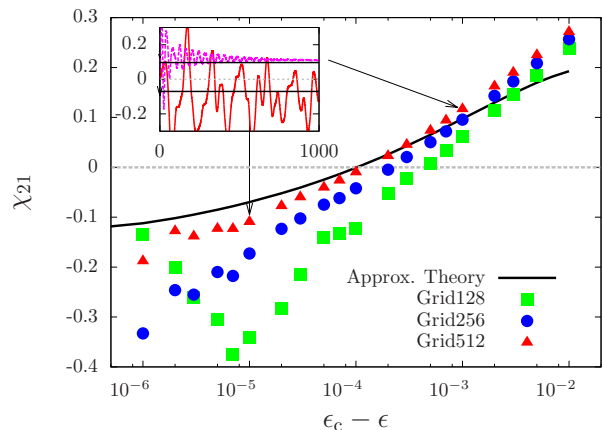


FIG. 6. The same with Fig.5, but we omitted χ_{11} and the vertical axis is in the linear scale to observe the negative part. (Inset) Temporal evolution of $\chi_{21}(t)$ in the interval $t \in [0, 1000]$. The upper magenta and the lower red lines are for $\epsilon_c - \epsilon = 10^{-3}$ and 10^{-5} , respectively, with the approximate theoretical levels (black solid lines).

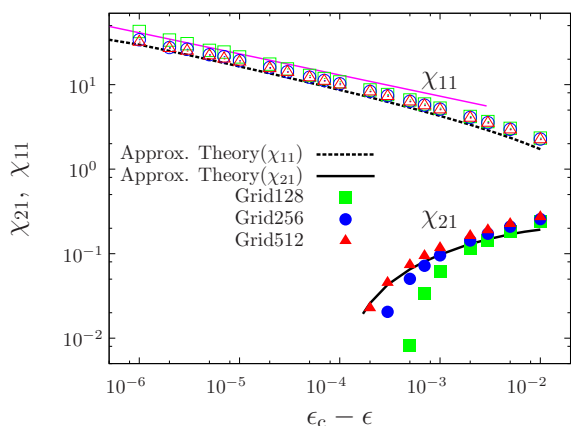


FIG. 5. Time averaged χ_{11} (open symbols) and χ_{21} (filled symbols) in the Ferro side of the Para-Ferro phase transitions. $h_1 = 10^{-5}$ and $h_2 = 0$. The averages are taken in the time window $[200, 1000]$. The grid size is $G = 128$ (green squares), 256 (blue circles) and 512 (red triangles). The black dashed and the black solid lines are susceptibilities from an approximate theory for χ_{11} and χ_{21} respectively. The magenta straight line is a guide of eyes for the slope $-1/4$.

C. $\chi_{21}^V(\text{FP}) < 0$ close to the critical point

The susceptibility χ_{21} in Fig.5 is hidden close to the critical point, since χ_{21} becomes negative. The negative susceptibility is confirmed as shown in Fig.6 by taking the linear scale for the vertical axis. This observation in the Vlasov dynamics gives a sharp contrast with in thermal equilibrium, in which the susceptibility χ_{21}^c is positive and diverges at the critical point.

VI. SUMMARY AND DISCUSSIONS

We considered responses to the external fields in the GHMF model. This model has the two order parameters, which characterize the Para, the Ferro and the Nematic phases. In each of thermal equilibrium and of the Vlasov dynamics, we derived 6 critical exponent matrices corresponding to the two sides of the three phase transitions, where each critical exponent matrix is of 2×2 associated with the two order parameters and their conjugate external fields.

As in the HMF model, the Para phase in the Vlasov dynamics has the same critical exponent matrices with thermal equilibrium. This agreement comes from the fact that both $\langle \cos aq \rangle_0$ and $\langle \cos aq \rangle_{H_0}$ vanish in the Para phase and no dynamical effects appear in the matrix D^V . In the Ferro side of the Para-Ferro phase transition, and the Nematic side of the Para-Nematic phase transition, we obtained the suppressed critical exponent $\gamma = 1/4$ as the straightforward extension from the HMF model, where $\gamma = 1$ in statistical mechanics. However, in the Ferro and the Nematic phases, all the other exponents are zeros, and no divergences of susceptibility appear at the critical points. The vanishing critical exponents in the Vlasov dynamics are stronger suppression than the reduced value of the previously mentioned $\gamma = 1/4$. These theoretical predictions of no divergences are successfully confirmed by direct numerical simulations of the Vlasov dynamics.

We found two types of nondivergences of susceptibilities: one appears in $\chi_{11}^V(\text{NF})$ and $\chi_{11}^V(\text{FN})$, and the other in the off-diagonal elements of $\chi^V(\text{FP})$. The former type might be understood by the potential barrier formed spontaneously by m_{20} . Around the critical point, the potential is $V_0 \approx -\Lambda_2 m_{20} \cos 2q$, and has the two wells centered at $q = 0$ (well-1) and $q = \pi$ (well-2). Applying the external field to

the direction of $q = 0$, particles in the well-2 tend to move to the well-1, but the potential barrier may prevent them from moving, since each particle must conserve energy in the Vlasov dynamics. On the other hand, in the latter type, the nondivergences comes from the domination of $O(\sqrt{m_{10}})$ in the off-diagonal elements of the matrix D^V , but the thermal equilibrium case also have the leading $O(m_{10})$ terms in the off-diagonal elements of the matrix D^c . Thus, the mechanism might not be straightforward comparing with the former type.

We remark that a non-divergent susceptibility is reported in the HMF model with a family of spatially homogeneous but asymmetric momentum distributions [32] at the point of stability change. The thermal equilibrium states, discussed in the present article, are symmetric and accept non-homogeneous distributions, and hence the reported non-divergences might have a larger impact than the asymmetric case.

We also revealed that negative elements appear in the susceptibility matrix for the Ferro side of the Para-Ferro phase transition. The negative susceptibility has been reported in the HMF model [34–36] and in the ϕ^4 model [4, 37], but they appear under the energy conservation between with and without the external field [34] (see also Appendix B), the fixed value of magnetization [4, 37], or the nonstationary initial states [35, 36]. The negative susceptibility reported in this article is observed for the initial thermal equilibrium states by applying an external field without any additional constraints, and therefore, it might be rather easy to compare with experiments.

Finally, it might be worth noting that the nonclassical critical exponents of the HMF model are also observed in a model of coupled oscillators by setting the so-called natural frequencies deterministically [38]. In the model, the oscillators are confined on the unit circle and the interaction is realized only through the first Fourier mode as the HMF model. Thus, it might be interesting to consider a similar extension in the coupled oscillator system.

ACKNOWLEDGMENTS

Y.Y.Y. thanks S.Ogawa for valuable discussions. He acknowledges the supports of JSPS KAKENHI Grant Numbers 23560069 and 16K05472.

Appendix A: Estimations of m_{a0}

Around the critical point, we estimate the spontaneous order parameters m_{a0} 's, which are written as

$$m_{a0} = \frac{\int_{-\pi}^{\pi} \exp[\beta(\Lambda_1 m_{10} \cos q + \Lambda_2 m_{20} \cos 2q)] \cos a q dq}{\int_{-\pi}^{\pi} \exp[\beta(\Lambda_1 m_{10} \cos q + \Lambda_2 m_{20} \cos 2q)] dq}, \quad (\text{A1})$$

where the denominator is of $O(1)$. The key idea of this section is to use the orthogonality of $\{\cos a q\}_{a \in \mathbb{Z}}$, which gives

$$\begin{aligned} m_{30} &= O(m_{10}^3) + O(m_{10} m_{20}), \\ m_{40} &= O(m_{10}^4) + O(m_{10}^2 m_{20}) + O(m_{20}^2). \end{aligned} \quad (\text{A2})$$

It is, therefore, enough to estimate m_{10} and m_{20} . We first consider the Para-Ferro and the Para-Nematic phase transitions, around which m_{10} and m_{20} are small enough, and then go to the Nematic-Ferro transition.

1. Para-Ferro and Para-Nematic transitions

All the order parameters are zeros in the Para phase, and we focus on estimating the order parameters in the Ferro and the Nematic sides.

The normalization factor, the numerator of the right-hand-side of (A1), is expanded as

$$\begin{aligned} &\int_{-\pi}^{\pi} \exp[\beta(\Lambda_1 m_{10} \cos q + \Lambda_2 m_{20} \cos 2q)] dq \\ &= 2\pi + O(m_{10}^2) + O(m_{20}^2). \end{aligned} \quad (\text{A3})$$

Thus, the self-consistent equations, which are $a = 1$ and 2 in (A1), are reduced to

$$\begin{aligned} m_{10} &= \frac{\beta \Lambda_1}{2} m_{10} + O(m_{10} m_{20}) + O(m_{10}^3) + \dots, \\ m_{20} &= \frac{\beta \Lambda_2}{2} m_{20} + O(m_{10}^2) + O(m_{10}^2 m_{20}) + O(m_{20}^3) + \dots. \end{aligned} \quad (\text{A4})$$

In the Ferro side of the Para-Ferro phase transition, the ordering is $O(m_{20}) \leq O(m_{10}^2)$ [23], and m_{10} is determined by the leading two terms as

$$\left(1 - \frac{\beta \Lambda_1}{2}\right) m_{10} + O(m_{10}^3) = 0. \quad (\text{A5})$$

As assumed at the head of Sec.III C, the coefficient of the first term is of $O(\tau)$. Thus, we obtain $m_{10} = O(\tau^{1/2})$ and $m_{20} = O(m_{10}^2) = O(\tau)$ from the second equation of (A4). Further, the estimations (A2) give $m_{30} = O(\tau^{3/2})$ and $m_{40} = O(\tau^2)$.

In the Nematic side of the Para-Nematic transition m_{10} is always zero, and m_{20} is determined by the equation

$$\left(1 - \frac{\beta \Lambda_2}{2}\right) m_{20} + O(m_{20}^3) = 0. \quad (\text{A6})$$

As discussed above, we have $m_{20} = O(\tau^{1/2})$. Further, $m_{30} = 0$ and $m_{40} = O(\tau)$ from (A2).

2. Nematic-Ferro transition

In the Nematic-Ferro transition m_{20} is of $O(1)$, and we need to estimate m_{10} . Smallness of m_{10} reduces the nor-

malization factor as

$$\begin{aligned} & \int_{-\pi}^{\pi} \exp[\beta(\Lambda_1 m_{10} \cos q + \Lambda_2 m_{20} \cos 2q)] dq \\ & \simeq \int_{-\pi}^{\pi} \exp(\beta \Lambda_2 m_{20} \cos 2q) dq + O(m_{10}^2). \end{aligned} \quad (\text{A7})$$

The self-consistent equation for m_{10} is expanded as

$$m_{10} = \frac{\beta \Lambda_1 m_{10}}{2} \left(1 + \frac{\int \exp(\beta \Lambda_2 m_{20} \cos 2q) \cos 2q dq}{\int \exp(\beta \Lambda_2 m_{20} \cos 2q) dq} \right) + O(m_{10}^3), \quad (\text{A8})$$

and the definition of m_{20} gives

$$\left[1 - \frac{\beta \Lambda_1 m_{10}}{2} (1 + m_{20}) \right] m_{10} + O(m_{10}^3) = 0 \quad (\text{A9})$$

where we used the fact

$$m_{20} = \frac{\int \exp[\beta \Lambda_2 m_{20} \cos 2q] \cos 2q dq}{\int \exp[\beta \Lambda_2 m_{20} \cos 2q] dq} + O(m_{10}^2). \quad (\text{A10})$$

Recalling the critical line (31), from (A9), we conclude that $m_{10} = O(\tau^{1/2})$. From (A2) we also estimate $m_{30} = O(\tau^{1/2})$ and $m_{40} = O(1)$.

Appendix B: Critical exponents in microcanonical ensemble

In the microcanonical ensemble, temperature may be modified by applying an external field \mathbf{h} at the time $t = 0$ due to the energy conservation. Denoting the modified temperature by T^{mc} , we consider the energy conservation relation between $t = 0^+$ and $t \rightarrow \infty$ as

$$\begin{aligned} & \frac{T}{2} + \frac{1 - \Lambda_1 m_{10}^2 - \Lambda_2 m_{20}^2}{2} - h_1 m_{10} - h_2 m_{20} \\ & = \frac{T^{\text{mc}}}{2} + \frac{1 - \Lambda_1 (m_1^{\text{mc}})^2 - \Lambda_2 (m_2^{\text{mc}})^2}{2} - h_1 m_1^{\text{mc}} - h_2 m_2^{\text{mc}} \end{aligned} \quad (\text{B1})$$

where m_1^{mc} and m_2^{mc} are the values of order parameters in the microcanonical ensemble. Introducing the response

$$\delta \mathbf{m}^{\text{mc}} = \begin{pmatrix} m_1^{\text{mc}} - m_{10} \\ m_2^{\text{mc}} - m_{20} \end{pmatrix}, \quad (\text{B2})$$

which will be determined later, the above relation gives the shift of inverse temperature from β to $\beta + \delta\beta$, where

$$\delta\beta \simeq -2\beta^2 \mathbf{m}_0^{\text{T}} \Lambda \delta \mathbf{m}^{\text{mc}} \quad (\text{B3})$$

up to the leading order.

Let us introduce the vectors

$$\mathbf{m}_0 = \begin{pmatrix} m_{10} \\ m_{20} \end{pmatrix}, \quad \mathbf{c}(q) = \begin{pmatrix} \cos q \\ \cos 2q \end{pmatrix} \quad (\text{B4})$$

and the discrepancy of potential

$$\delta V^{\text{mc}} = -\mathbf{c}^{\text{T}} \Lambda \delta \mathbf{m}^{\text{mc}} - \mathbf{c}^{\text{T}} \mathbf{h}. \quad (\text{B5})$$

The self-consistent equation in the microcanonical ensemble is obtained by replacing $\beta\delta V^{\text{c}}$ with $\beta\delta V^{\text{mc}} + H_0\delta\beta$ in (20),

$$\delta \mathbf{m}^{\text{mc}} = -\langle \mathbf{c}(\beta\delta V^{\text{mc}} + H_0\delta\beta) \rangle_0 + \langle \mathbf{c} \rangle_0 \langle \beta\delta V^{\text{mc}} + H_0\delta\beta \rangle_0. \quad (\text{B6})$$

Noting that $p^2/2$ term of H_0 is canceled between the two terms, and substituting (B3), (B5) and

$$V_0 = -\mathbf{c}^{\text{T}} \Lambda \mathbf{m}_0 \quad (\text{B7})$$

into the self-consistent equation (B6), we have

$$\delta \mathbf{m}^{\text{mc}} = \beta C^{\text{c}} (\mathbb{1}_2 - 2\beta \Lambda \mathbf{m}_0 \mathbf{m}_0^{\text{T}}) \Lambda \delta \mathbf{m}^{\text{mc}} + \beta C^{\text{c}} \mathbf{h} \quad (\text{B8})$$

where $C^{\text{c}} = \langle \mathbf{c} \mathbf{c}^{\text{T}} \rangle_0$ by the definition. The response $\delta \mathbf{m}^{\text{mc}}$ in the microcanonical ensemble is, therefore,

$$\delta \mathbf{m}^{\text{mc}} = (D^{\text{mc}})^{-1} \beta C^{\text{c}} \mathbf{h}, \quad (\text{B9})$$

where the matrix D^{mc} is defined by

$$D^{\text{mc}} = \mathbb{1}_2 - \beta C^{\text{c}} (\mathbb{1}_2 - 2\beta \Lambda \mathbf{m}_0 \mathbf{m}_0^{\text{T}}) \Lambda. \quad (\text{B10})$$

The matrix D^{mc} is expressed as

$$D^{\text{mc}} = D^{\text{c}} + 2\beta^2 C^{\text{c}} \Lambda \mathbf{m}_0 \mathbf{m}_0^{\text{T}} \Lambda, \quad (\text{B11})$$

and the second term of the right-hand-side does not change the dominating τ dependence of D^{mc} from D^{c} . This concludes that the critical exponents are shared between the canonical and the microcanonical ensembles.

We give a remark on usage of the energy conservation. If we require the energy conservation between $t = 0^-$ and $t \rightarrow \infty$, the energy conservation relation is modified from (B1) to

$$\begin{aligned} & \frac{T}{2} + \frac{1 - \Lambda_1 m_{10}^2 - \Lambda_2 m_{20}^2}{2} \\ & = \frac{T^{\text{ene}}}{2} + \frac{1 - \Lambda_1 (m_1^{\text{ene}})^2 - \Lambda_2 (m_2^{\text{ene}})^2}{2} - h_1 m_1^{\text{ene}} - h_2 m_2^{\text{ene}} \end{aligned} \quad (\text{B12})$$

where all the superscripts are replaced to represent the considering situation. Then, $\delta\beta$ is modified to

$$\delta\beta^{\text{ene}} \simeq -2\beta^2 \mathbf{m}_0^{\text{T}} (\Lambda \delta \mathbf{m}^{\text{ene}} + \mathbf{h}). \quad (\text{B13})$$

In the previous setting, the last term was not proportional to $\mathbf{m}_0^{\text{T}} \mathbf{h}$ but to $\delta \mathbf{m}^{\text{T}} \mathbf{h}$ and was omitted since it was of higher order. With the modified $\delta\beta^{\text{ene}}$, we have the linear response $\delta \mathbf{m}^{\text{ene}}$ as

$$\delta \mathbf{m}^{\text{ene}} = (D^{\text{mc}})^{-1} \beta C^{\text{c}} (\mathbb{1}_2 - 2\beta \Lambda \mathbf{m}_0 \mathbf{m}_0^{\text{T}}) \mathbf{h}. \quad (\text{B14})$$

Divergences of the linear response come from $(D^{\text{mc}})^{-1}$ again, and hence the critical exponents are not modified. On the other hand, the response $\delta \mathbf{m}^{\text{ene}}$ may be negative in the off-diagonal elements due to the factor $\mathbb{1}_2 - 2\beta \Lambda \mathbf{m}_0 \mathbf{m}_0^{\text{T}}$, and even in the diagonal elements for large β , which implies large \mathbf{m}_0 .

Appendix C: Integral formula for elements of the matrix B^V in a reduced case

We give a useful formula of the matrix B^V in the case that the one-particle Hamiltonian is written in the form

$$H_0(q, p) = \frac{p^2}{2} - M \cos q, \quad (M > 0). \quad (C1)$$

This form includes the Nematic phase by replacing q with $2q$ and setting $M = \Lambda_2 m_{20}$, and the approximate theory used in Sec.VB, which is for the Ferro side of the Para-Ferro phase transition, by setting $m_{20} = 0$ and $M = \Lambda_1 m_{10}$. We note that this Hamiltonian is symmetric with respect to both q and p , namely $H_0(-q, p) = H_0(q, -p) = H_0(q, p)$. We will use this symmetry for reducing computations.

1. Angle-action variables and elliptic integrals

The Hamiltonian system H_0 (C1) is integrable, and we can introduce the associated angle-action variables (θ, J) . They are written in the use of the Legendre elliptic integrals, defined by

$$F(\phi, k) = \int_0^\phi \frac{d\varphi}{\sqrt{1 - k^2 \sin^2 \varphi}} = \int_0^{\sin \phi} \frac{du}{\sqrt{(1 - u^2)(1 - k^2 u^2)}} \quad (C2)$$

and

$$E(\phi, k) = \int_0^\phi \sqrt{1 - k^2 \sin^2 \varphi} d\varphi = \int_0^{\sin \phi} \sqrt{\frac{1 - k^2 u^2}{1 - u^2}} du. \quad (C3)$$

The complete elliptic integrals of the first and the second kinds are defined respectively as

$$K(k) = F(\pi/2, k), \quad E(k) = E(\pi/2, k). \quad (C4)$$

The Hamiltonian system H_0 (C1) has two hyperbolic fixed points, $(q, p) = (-\pi, 0)$ and $(\pi, 0)$, and they are connected by the separatrix. The phase space μ is divided into outside and inside of the separatrix. See Fig.1(a) for a schematic picture of the phase space. Based on this knowledge, the angle-action variables (θ, J) are introduced as [33]

$$J = \begin{cases} \frac{4\sqrt{M}}{\pi} kE(1/k) & \text{separatrix outside} \\ \frac{8\sqrt{M}}{\pi} [E(k) - (1 - k^2)K(k)] & \text{separatrix inside} \end{cases} \quad (C5)$$

and

$$\theta = \begin{cases} \frac{F(q/2, 1/k)}{\pi \frac{K(1/k)}{K(k)}} & \text{separatrix outside, upper-half} \\ \frac{\pi F(Q, k)}{2 \frac{K(k)}{K(1/k)}} & \text{separatrix inside, upper-half} \\ \frac{\pi}{2} \left(2 - \frac{F(Q, k)}{K(k)} \right) & \text{separatrix inside, lower-half} \\ -\pi \frac{F(q/2, 1/k)}{K(1/k)} & \text{separatrix outside, lower-half} \end{cases} \quad (C6)$$

where

$$k = \sqrt{\frac{H_0(q, p) + M}{2M}} \quad (C7)$$

and Q is defined by

$$k \sin Q = \sin(q/2). \quad (C8)$$

The energy minimum corresponds to $k = 0$, and the separatrix energy to $k = 1$.

For later convenience, we introduce the integrals

$$N_n(k) = \int_0^1 \frac{u^n du}{\sqrt{(1 - u^2)(1 - k^2 u^2)}}. \quad (C9)$$

This integrals have the recursive formula

$$(m+2)k^2 N_{m+3}(k) - (m+1)(1+k^2)N_{m+1}(k) + mN_{m-1}(k) = 0, \quad (C10)$$

and hence

$$\begin{aligned} N_0(k) &= K(k), \\ N_2(k) &= \frac{K(k) - E(k)}{k^2}, \\ N_4(k) &= \frac{(2+k^2)K(k) - 2(1+k^2)E(k)}{3k^4}. \end{aligned} \quad (C11)$$

2. Computations of $\langle \cos bq \rangle_{H_0}$

Let us compute the averages

$$\langle \cos^n q \rangle_{H_0} = \frac{1}{2\pi} \int_{-\pi}^{\pi} \cos^n q(\theta, J) d\theta. \quad (C12)$$

Using the elliptic function sn, which is the inverse function of $F(\phi, k)$ and is defined by

$$\text{sn}(F(\phi, k), k) = \sin \phi, \quad (C13)$$

we can write $\cos q$ as [24]

$$\cos q = \begin{cases} 1 - 2\text{sn}^2 \left(\frac{K(1/k)}{\pi} \theta, \frac{1}{k} \right) & \text{separatrix outside,} \\ 1 - 2k^2 \text{sn}^2 \left(\frac{2K(k)}{\pi} \theta, k \right) & \text{separatrix inside.} \end{cases} \quad (C14)$$

Changing the variable as

$$\theta = \begin{cases} \frac{\pi}{K(1/k)} F(\phi, 1/k) & \text{separatrix outside,} \\ \frac{\pi}{2K(k)} F(\phi, k) & \text{separatrix inside,} \end{cases} \quad (C15)$$

and using the symmetry of $H_0(q, p)$, we have the expressions of $\langle \cos^n q \rangle_{H_0}$ as

$$\langle \cos^n q \rangle_{H_0} = \begin{cases} \frac{1}{K(1/k)} \int_0^1 \frac{(1-2u^2)^n}{\sqrt{(1-u^2)(1-k^{-2}u^2)}} du & \text{separatrix outside,} \\ \frac{1}{K(k)} \int_0^1 \frac{(1-2k^2u^2)^n}{\sqrt{(1-u^2)(1-k^2u^2)}} du & \text{separatrix inside.} \end{cases} \quad (C16)$$

Thus, the integrals $N_n(k)$, (C11), derive $\langle \cos q \rangle_{H_0}$ and $\langle \cos^2 q \rangle_{H_0}$. The concrete expressions of $\langle \cos q \rangle_{H_0}$ and $\langle \cos 2q \rangle_{H_0}$, which can be computed from $\langle \cos^2 q \rangle_{H_0}$, are

$$\langle \cos q \rangle_{H_0} = \begin{cases} 2k^2 \frac{E(1/k)}{K(1/k)} - (2k^2 - 1) & \text{separatrix outside,} \\ 2 \frac{E(k)}{K(k)} - 1 & \text{separatrix inside,} \end{cases} \quad (\text{C17})$$

and

$$\langle \cos 2q \rangle_{H_0} = \begin{cases} \frac{8k^2}{3}(1-2k^2) \frac{E(1/k)}{K(1/k)} + 1 - \frac{16k^2}{3}(1-k^2) & \text{separatrix outside,} \\ \frac{8}{3}(1-2k^2) \frac{E(k)}{K(k)} - \frac{5-8k^2}{3} & \text{separatrix inside.} \end{cases} \quad (\text{C18})$$

3. Computations of $\langle \langle \cos aq \rangle_{H_0} \langle \cos bq \rangle_{H_0} \rangle_0$

We first show the equality (50). Noting that f_0 and $\langle \psi_2 \rangle_{H_0}$ depends on J only, and using $dqdp = d\theta dJ$, we can show

$$\begin{aligned} \langle \psi_1 \langle \psi_2 \rangle_{H_0} \rangle_0 &= \int dJ f_0 \langle \psi_2 \rangle_{H_0} \int d\theta \psi_1 \\ &= 2\pi \int dJ f_0 \langle \psi_2 \rangle_{H_0} \langle \psi_1 \rangle_{H_0} = \iint_{\mu} f_0 \langle \psi_1 \rangle_{H_0} \langle \psi_2 \rangle_{H_0} dqdp \\ &= \langle \langle \psi_1 \rangle_{H_0} \langle \psi_2 \rangle_{H_0} \rangle_0. \end{aligned} \quad (\text{C19})$$

We then consider the average

$$\langle \langle \cos aq \rangle_{H_0} \langle \cos bq \rangle_{H_0} \rangle_0 = 2\pi \int f_0 \langle \cos aq \rangle_{H_0} \langle \cos bq \rangle_{H_0} dJ. \quad (\text{C20})$$

As shown previously, the average $\langle \cos aq \rangle_{H_0}$ is obtained as a function of k , and accordingly, we change the integral variable from J to k by using the Jacobian

$$\frac{dJ}{dk} = \begin{cases} \frac{4\sqrt{M}}{\pi} K(1/k) & \text{separatrix outside,} \\ \frac{8\sqrt{M}}{\pi} kK(k) & \text{separatrix inside,} \end{cases} \quad (\text{C21})$$

where we used the derivatives of $K(k)$ and $E(k)$

$$\begin{aligned} \frac{dK}{dk}(k) &= \frac{E(k) - (1-k^2)K(k)}{k(1-k^2)}, \\ \frac{dE}{dk}(k) &= \frac{E(k) - K(k)}{k}. \end{aligned} \quad (\text{C22})$$

Denoting the initial stationary state as $f_0(q, p) = G_0(k)$, and recalling that the separatrix outside has two contributions

from the upper and the lower of the separatrix, we have

$$\begin{aligned} &\langle \langle \cos aq \rangle_{H_0} \langle \cos bq \rangle_{H_0} \rangle_0 \\ &= 16\sqrt{M} \int_1^\infty G_0(k) K(1/k) \langle \cos aq \rangle_{H_0} \langle \cos bq \rangle_{H_0} dk \\ &+ 16\sqrt{M} \int_0^1 G_0(k) kK(k) \langle \cos aq \rangle_{H_0} \langle \cos bq \rangle_{H_0} dk. \end{aligned} \quad (\text{C23})$$

4. The (1, 1)-element in the Nematic phase

We give the (1, 1)-element in the Nematic phase. We derive it via replacing q with $2q$ in the obtained results. We note that the same formula is also derived by starting from the Hamiltonian

$$H_0 = \frac{p^2}{2} - \Lambda_2 m_{20} \cos 2q. \quad (\text{C24})$$

The Nematic phase has two hyperbolic fixed points of $(q, p) = (-\pi/2, 0)$ and $(\pi/2, 0)$ and the separatrix connects them by forming two ‘‘eyes’’ centered at $(q, p) = (0, 0)$ (eye-1) and $(\pi, 0)$ (eye-2). See Fig.1(b).

From symmetry, the average $\langle \cos q \rangle_{H_0}$ is canceled in separatrix outside. Indeed, the average is modified as

$$\begin{aligned} 2\pi \langle \cos aq \rangle_{H_0} &= \int_0^{2\pi} \cos aq(\theta) d\theta = \int_0^{2\pi} \cos aq(\theta + \pi) d\theta \\ &= \int_0^{2\pi} \cos a(q(\theta) + \pi) d\theta = \cos a\pi \times 2\pi \langle \cos aq \rangle_{H_0}. \end{aligned} \quad (\text{C25})$$

In the eye inside, we have the transform

$$\cos q = \begin{cases} \sqrt{\frac{1 + \cos 2q}{2}} & q \in (-\pi/2, \pi/2): \text{eye-1} \\ -\sqrt{\frac{1 + \cos 2q}{2}} & q \in (-\pi, -\pi/2) \cup (\pi/2, \pi): \text{eye-2} \end{cases} \quad (\text{C26})$$

and, referring to (C14), $\cos 2q$ is expressed as

$$\cos 2q = 1 - 2k^2 \text{sn}^2 \left(\frac{2K(k)}{\pi} \theta, k \right). \quad (\text{C27})$$

Therefore, we totally have

$$\langle \cos q \rangle_{H_0} = \begin{cases} 0 & \text{separatrix outside,} \\ \frac{\pi}{2K(k)} & \text{eye-1 inside.} \\ -\frac{\pi}{2K(k)} & \text{eye-2 inside.} \end{cases} \quad (\text{C28})$$

We have two contributions from the eye-1 and the eye-2, but the factor 2 is canceled with the factor 1/2 from the Jacobian dJ/dk . Indeed, the action variable defined as

$$J = \oint pdq \quad (\text{C29})$$

becomes half since the traveling distance of a periodic orbit becomes half in the separatrix inside of Fig.1(b) comparing

with Fig.1(a). We remark that the action in the separatrix outside does not change since the traveling distance does not change.

Putting all together with the thermal equilibrium state

$$f_0(q, p) = \frac{e^{-\beta(p^2/2 - M \cos 2q)}}{\iint_{\mu} e^{-\beta(p^2/2 - M \cos 2q)} dq dp} = \frac{e^{-\beta M(2k^2 - 1)}}{\sqrt{2\pi/\beta} 2\pi I_0(\beta M)}, \quad (\text{C30})$$

we have

$$\langle \langle \cos q \rangle_{H_0} \langle \cos q \rangle_{H_0} \rangle_0 = \frac{\sqrt{2\pi\beta M}}{I_0(\beta M)} \int_0^1 e^{-\beta M(2k^2 - 1)} \frac{k}{K(k)} dk. \quad (\text{C31})$$

This expression results to $B_{11}^V(\text{NF})$ (61) by setting $M = \Lambda_2 m_{20}$.

Appendix D: Estimations of B^V matrix

We give estimations of the matrix B^V (52) by using the formula (C23), which implies $B^V = O(\sqrt{M})$ by appropriately setting M , since the integral part does not vanish even in the limit $M \rightarrow 0$. Keeping this ordering in mind, we separately discuss on the Para, the Nematic and the Ferro phases.

1. Para phase

All the order parameters are zeros in the Para phase, and the angle variable is nothing but q . Thus, we have $\langle \cos aq \rangle_{H_0} = 0$ and hence

$$B^V(\text{PF}) = \begin{pmatrix} 0 & 0 \\ 0 & 0 \end{pmatrix}, \quad B^V(\text{PN}) = \begin{pmatrix} 0 & 0 \\ 0 & 0 \end{pmatrix}. \quad (\text{D1})$$

This is consistent with setting $M = 0$ in the formula (C23).

2. Nematic phase

The parameter M is regarded as $\Lambda_2 m_{20}$, and the matrices B^V is of $O(m_{20})$. However, the off-diagonal elements vanish due to cancellation. The cancellation can be found as follows. In separatrix outside, we recall $\langle \cos q \rangle_{H_0} = 0$ and there is no contribution from the separatrix outside to the

off-diagonal elements. In separatrix inside, we have contributions from two eyes (see the Appendix C4). The contribution from the eye-2 is obtained by shifting the variable q with π in the contribution from the eye-1, and is multiplied by $\cos a\pi$. Thus, the total contribution from the two eyes has the prefactor $1 + \cos a\pi \cos b\pi$, and vanishes for $(a, b) = (1, 2)$ and $(2, 1)$. The ordering of m_{20} is $m_{20} = O(\tau^{1/2})$ for the Para-Nematic phase transition, and $m_{20} = O(1)$ for the Nematic-Ferro phase transition. These estimations give

$$B^V(\text{NP}) = \begin{pmatrix} O(\tau^{1/4}) & 0 \\ 0 & O(\tau^{1/4}) \end{pmatrix}, \quad B^V(\text{NF}) = \begin{pmatrix} O(1) & 0 \\ 0 & O(1) \end{pmatrix}. \quad (\text{D2})$$

3. Ferro phase

For the Para-Ferro phase transition, we may approximate the potential as

$$V_0 \simeq -\Lambda_1 m_{10} \cos q, \quad (\text{D3})$$

and hence the parameter M is regarded as $\Lambda_1 m_{10}$ and is of $O(\tau^{1/2})$. There is no reason of cancellation which occurs in the Nematic phase, and hence we have

$$B^V(\text{FP}) = \begin{pmatrix} O(\tau^{1/4}) & O(\tau^{1/4}) \\ O(\tau^{1/4}) & O(\tau^{1/4}) \end{pmatrix}. \quad (\text{D4})$$

For the Nematic-Ferro phase transition, we may approximate the potential as

$$V_0 \simeq -\Lambda_2 m_{20} \cos 2q, \quad (\text{D5})$$

and hence the parameter M is regarded as $\Lambda_2 m_{20}$ and is of $O(1)$. The approximated potential is the same with one in the Nematic phase, but the cancellation does not exactly occur by symmetry breaking due to non-zero m_{10} . The off-diagonal elements may be non-zeros and tend to vanish as approaching to the critical line. However, the off-diagonal elements are not important to observe nondivergence of susceptibility at the critical point of the Nematic-Ferro phase transition, and we skip the precise computations. Consequently, we have

$$B^V(\text{FN}) = \begin{pmatrix} O(1) & O(\tau^{c_1}) \\ O(\tau^{c_2}) & O(1) \end{pmatrix} \quad (\text{D6})$$

with $c_1, c_2 > 0$.

[1] L. Landau, On the theory of phase transitions, Zh. Eksp. Teor. Fiz. **7**, 19 (1937).
[2] A. Campa, A. Giansanti and D. Moroni, Canonical solution of a system of long-range interacting rotators on a lattice, Phys. Rev. E **62**, 303 (2000).
[3] T. Mori, Analysis of the exactness of mean-field theory in long-range interacting systems, Phys. Rev. E **82**, 060103(R) (2010).

[4] A. Campa, T. Dauxois and S. Ruffo, Statistical mechanics and dynamics of solvable models with long-range interactions, Phys. Rep. **480**, 57 (2009).
[5] W. Braun and K. Hepp, The Vlasov Dynamics and Its Fluctuations in the $1/N$ Limit of Interacting Classical Particles, Commun. Math. Phys. **56**, 101 (1977).
[6] R. L. Dobrushin, Vlasov equations, Funct. Anal. Appl. **13**, 115 (1979).

- [7] H. Neunzert, An introduction to the nonlinear Boltzmann-Vlasov equation, in *Kinetic Theories and the Boltzmann Equation*, ed. by C. Cercignani, pp.60-110. Lecture Notes in Mathematics 1048 (Springer, Berlin, Heidelberg, 1984).
- [8] H. Spohn, *Large Scale Dynamics of Interacting Particles* (Springer, Heidelberg, 1991).
- [9] D. H. Zanette and M. A. Montemurro, Dynamics and nonequilibrium states in the Hamiltonian mean-field model: A closer look, *Phys. Rev. E* **67**, 031105 (2003).
- [10] Y. Y. Yamaguchi, J. Barré, F. Bouchet, T. Dauxois and S. Ruffo, Stability criteria of the Vlasov equation and quasi-stationary states of the HMF model, *Physica A* **337**, 36 (2004).
- [11] J. Barré, F. Bouchet, T. Dauxois, S. Ruffo and Y. Y. Yamaguchi, The Vlasov equation and the Hamiltonian mean-field model, *Physica A* **365**, 177 (2006).
- [12] L. G. Moyano and C. Anteneodo, Diffusive anomalies in a long-range Hamiltonian system, *Phys. Rev. E* **74**, 021118 (2006).
- [13] K. Jain, F. Bouchet and D. Mukamel, Relaxation times of unstable states in systems with long range interactions, *J. Stat. Mech.* (2007) P11008.
- [14] P. de Buyl, D. Mukamel and S. Ruffo, Self-consistent inhomogeneous steady states in Hamiltonian mean-field dynamics, *Phys. Rev. E* **84**, 061151 (2011).
- [15] P. H. Chavanis, Kinetic theory of spatially homogeneous systems with long-range interactions: I. General results, *Eur. Phys. J. Plus* **127**, 19 (2012).
- [16] P. Mazur, NON-ERGODICITY OF PHASE FUNCTIONS IN CERTAIN SYSTEMS, *Physica (Amsterdam)* **43**, 533 (1969).
- [17] M. Suzuki, ERGODICITY, CONSTANTS OF MOTION, AND BOUNDS FOR SUSCEPTIBILITIES, *Physica (Amsterdam)* **51**, 277 (1971).
- [18] S. Inagaki and T. Konishi, Dynamical Stability of a Simple Model Similar to Self-Gravitating Systems, *Publ. Astron. Soc. Japan* **45**, 733 (1993).
- [19] M. Antoni and S. Ruffo, Clustering and relaxation in Hamiltonian long-range dynamics, *Phys. Rev. E* **52**, 2361 (1995).
- [20] A. Patelli, S. Gupta, C. Nardini and S. Ruffo, Linear response theory for long-range interacting systems in quasistationary states, *Phys. Rev. E* **85**, 021133 (2012).
- [21] S. Ogawa and Y. Y. Yamaguchi, Linear response theory in the Vlasov equation for homogeneous and for inhomogeneous quasistationary states, *Phys. Rev. E* **85**, 061115 (2012).
- [22] S. Ogawa, A. Patelli and Y. Y. Yamaguchi, Non-mean-field critical exponent in a mean-field model: Dynamics versus statistical mechanics, *Phys. Rev. E* **89**, 032131 (2014).
- [23] S. Ogawa and Y. Y. Yamaguchi, Landau-like theory for universality of critical exponents in quasistationary states of isolated mean-field systems, *Phys. Rev. E* **91**, 062108 (2015).
- [24] S. Ogawa and Y. Y. Yamaguchi, Nonlinear response for external field and perturbation in the Vlasov system, *Phys. Rev. E* **89**, 052114 (2014).
- [25] Y. Y. Yamaguchi, Strange scaling and relaxation of finite-size fluctuation in thermal equilibrium, *Phys. Rev. E* **94**, 012133 (2016).
- [26] R. Botet, R. Jullien and P. Pfeuty, Size Scaling for Infinitely Coordinated Systems, *Phys. Rev. Lett.* **49**, 478 (1982).
- [27] R. Botet and R. Jullien, Large-size critical behavior of infinitely coordinated systems, *Phys. Rev. B* **28**, 3955 (1983).
- [28] T. N. Teles, F. P. da C. Benetti, R. Pakter and Y. Levin, Nonequilibrium Phase Transitions in Systems with Long-Range Interactions, *Phys. Rev. Lett.* **109**, 230601 (2012).
- [29] A. Pikovskiy, S. Gupta, T. N. Teles, F. P. C. Benetti, R. Pakter, Y. Levin and S. Ruffo, Ensemble inequivalence in a mean-field XY model with ferromagnetic and nematic couplings, *Phys. Rev. E* **90**, 062141 (2014).
- [30] Y. Y. Yamaguchi and S. Ogawa, Conditions for predicting quasistationary states by rearrangement formula, *Phys. Rev. E* **92**, 042131 (2015).
- [31] P. de Buyl, Numerical resolution of the Vlasov equation for the Hamiltonian Mean-Field model, *Commun. Nonlinear Sci. Numer. Simulat.* **15**, 2133 (2010).
- [32] Y. Y. Yamaguchi, Nondiagonalizable and nondivergent susceptibility tensor in the Hamiltonian mean-field model with asymmetric momentum distributions, *Phys. Rev. E* **92**, 032109 (2015).
- [33] J. Barré, A. Olivetti and Y. Y. Yamaguchi, Dynamics of perturbations around inhomogeneous backgrounds in the HMF model, *J. Stat. Mech.* (2010) P08002.
- [34] P. H. Chavanis, Thermodynamics of the HMF model with a magnetic field, *Eur. Phys. J. B* **80**, 275 (2011).
- [35] G. De Ninno and D. Fanelli, Out-of-equilibrium statistical ensemble inequivalence, *Eur. Phys. Lett.* **97**, 20002 (2012).
- [36] P. de Buyl, D. Fanelli and S. Ruffo, Phase transitions of quasistationary states in the Hamiltonian Mean Field model, *Cent. Eur. J. Phys.* **10**, 652 (2012).
- [37] A. Campa, S. Ruffo and H. Touchette, Negative magnetic susceptibility and nonequivalent ensembles for the mean-field ϕ^4 spin model, *Physica A* **385**, 233 (2007).
- [38] H. Hong, H. Chaté, L.-H. Tang and H. Park, Finite-size scaling, dynamic fluctuations, and hyperscaling relation in the Kuramoto model, *Phys. Rev. E* **92**, 022122 (2015).